ACS EARTH AND SPACE CHEMISTRY

http://pubs.acs.org/journal/aesccq
Article

Favorable Environments for the Formation of Ferrocyanide, a Potentially Critical Reagent for Origins of Life

Zoe R. Todd,* Nicholas F. Wogan, and David C. Catling

Cite This: ACS Earth Space Chem. 2024, 8, 221−229
Read Online
ACCESS | Metrics & More | Article Recommendations | Supporting Information

ABSTRACT: Cyanide and its derivatives play important roles in prebiotic chemistry through a variety of possible mechanisms. In particular, cyanide has been shown to allow for the synthesis of ribonucleotides and amino acids. Although dissolved hydrogen cyanide can be lost as a gas or undergo hydrolysis reactions, cyanide can also potentially be stored and stockpiled as ferrocyanide ($Fe(CN)_6^{-4}$), which is more stable. Furthermore, ferrocyanide aids in some prebiotic synthetic reactions. Here, we investigate the formation rates and yields of ferrocyanide as a function of various environmental parameters, such as the pH, temperature, and concentration. We find that ferrocyanide formation rates and yields are optimal at slightly alkaline conditions (pH 8−9) and moderate temperatures (≈20−30 °C). Given the wide range of possible lake environments likely available on early Earth, our results help to constrain the environmental conditions that would favor cyanide- and ferrocyanide-based prebiotic chemistries. We construct lake box models and find that ferrocyanide may be able to form and reach significant concentrations for prebiotic chemistry on the time scale of years under favorable conditions.

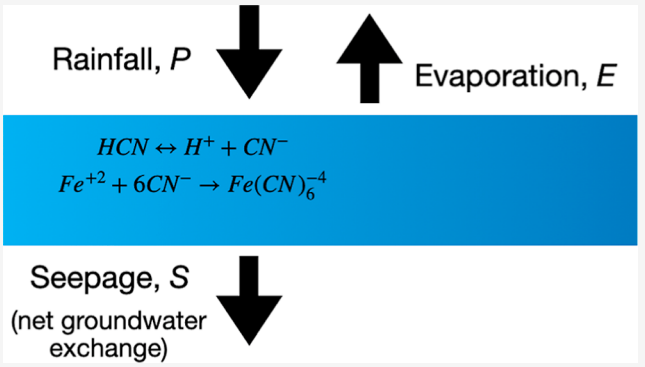

KEYWORDS: *ferrocyanide, prebiotic chemistry, early earth, origins of life, cyanide*

INTRODUCTION

Hydrogen cyanide and its derivatives have commonly been implicated in prebiotic syntheses of biomolecules. Oro[1] first demonstrated the synthesis of the nucleobase adenine from solutions of ammonium cyanide; furthermore, cyanide has historically been important in the synthesis of amino acids.[2,3] More recent "systems chemistry" approaches to prebiotic synthesis attempt to understand how a unified set of chemical reactions could lead to the generation of multiple classes of molecules needed for the origin of life. Substantial progress includes a common synthesis for amino acids, ribonucleotides, sugars, and lipid precursors from a cyanosulfidic chemistry.[4,5] Similarly, gamma irradiation of cyanide and simple, prebiotically plausible salts has been shown to generate sugars and RNA precursors.[6,7] Other suggestions for prebiotic syntheses make use of cyanide (e.g., Becker et al.,[8] Liu et al.,[9] Teichert et al.,[10] and Kim and Benner[11]), either as a source to make simple sugars and nitriles (e.g., formaldehyde and glycolonitrile) or through the HCN-driven synthesis of purines or formamidinopyrimidines. Thus, the importance of cyanide for prebiotic chemistry is not specific to one scenario, research group, or idea for the origins of life. Instead, decades of research have shown that cyanide is a robustly useful molecule in prebiotic synthesis.

Furthermore, cyanide is likely to have been available on the early Earth from a variety of sources, including atmospheric photochemistry,[12−15] lightning generation,[16,17] impact generation,[18−20] and impact delivery.[21] Estimates of the amounts of HCN available differ depending on the source as well as parameters including atmospheric composition.

Hydrogen cyanide can partition between the gas and the aqueous phases. Furthermore, HCN dissociates into the cyanide anion and a proton in aqueous solutions, with speciation set by the pH of the solution.

$$HCN_{(aq)} \leftrightarrow CN^-_{(aq)} + H^+_{(aq)} \quad (1)$$

Cyanide is not indefinitely stable in aqueous solutions; instead, it will undergo hydrolysis, first to formamide and then to formic acid (eq 2).

$$HCN + H_2O \rightarrow HCONH_2 \rightarrow HCOO^- + NH_4^+ \quad (2)$$

Received: July 19, 2023
Revised: January 7, 2024
Accepted: January 8, 2024
Published: February 1, 2024

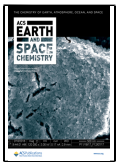

The rate of hydrolysis depends on the pH and temperature of the environment.[22] For prebiotic synthesis to occur, HCN must have sufficient concentrations and sufficient time for productive reactions. Given the range of sources of HCN, coupled with the varying hydrolysis rates and the unconstrained kinetics of some of the synthetic reactions, it is unclear if the degradation of HCN will limit prebiotic synthetic chemistry. If hydrolysis of HCN is faster than HCN can be delivered to an environment or if HCN is lost faster than it is used productively, bottlenecks on prebiotic synthesis might occur.

One alternative to this potential roadblock is that cyanide is stored in a more stable form, which can then be liberated for use in prebiotic chemistry later. For example, cyanide reacts with ferrous iron to form ferrocyanide ($Fe(CN)_6^{-4}$), which is more stable than cyanide itself

$$Fe(II) + 6CN^- \rightarrow [Fe(CN)_6^{4-}] \quad (3)$$

Ferrocyanide can store and stockpile cyanide,[23] which can then be liberated later through, e.g., thermal processing.[4] In addition, ferrocyanide has been shown to be useful for the prebiotic synthesis of the building blocks of life via reductive homologation of hydrogen cyanide.[5]

However, certain environments may decompose ferrocyanide. Near ultraviolet light (300−400 nm) degrades ferrocyanide via photoaquation; the time scale of this reaction depends on environmental conditions such as pH, temperature, and concentration.[24] The degradation of ferrocyanide is expected to be on the order of minutes to hours under typical planetary conditions,[24] which raises the important question of how quickly ferrocyanide can form. If ferrocyanide forms faster than it subsequently degrades, it can still be a plausible reactant for prebiotic chemistry. Thus, constraining the kinetics when ferrocyanide forms is important not only for understanding the plausibility of prebiotic chemistry that uses ferrocyanide but also for the potential stockpiling of cyanide in a more stable form. Past studies have focused primarily on the thermodynamics of ferrocyanide formation,[25,26] while assuming that the formation reaction is fast on geological time scales. While this assumption may be true, relevant time scales require an understanding of the kinetics of productive and destructive reactions of ferrocyanide to better assess the plausibility of suggested prebiotic chemical pathways.

In this study, we have measured the rates and yields of ferrocyanide formation at a number of pH values, temperatures, and concentrations of reagents. We use these experimental results to construct toy box models of lakes to assess the plausible concentrations and time scales of ferrocyanide production under various planetary conditions. We discuss our results and findings for planetary conditions to constrain which environments may be the most favorable for ferrocyanide accumulation.

RESULTS

When solutions of Fe(II) and cyanide are mixed together, an absorption feature with a maximum near 217 nm develops, which indicates the presence and concentration of ferrocyanide. Figure 1 shows the increase in ferrocyanide concentration, calculated from the absorbance maximum at 217 nm, after the reaction is initiated for pH-unadjusted (pH ≈ 10) 0.1 mM Fe(II) + 0.6 mM ΣHCN, at a temperature T = 25 °C. Here, ΣHCN is the sum of the concentrations of HCN and CN^-, where the partitioning between these species is set by the pH of the solution. We chose these concentrations because they are thought to be prebiotically relevant and are in the linear detection regime of the UV−vis spectrophotometer. The kinetics of the reaction are complicated: it is unclear what the order of the reaction is in either reactant (see Keefe and Miller[25]), and we do not use either reactant in excess, which would simplify the kinetic analysis. Therefore, we have chosen to quantify the change in ferrocyanide concentration with time over the first ten s of the reaction, which is an approximately linear increase (Figure 1B). Reactions appeared to reach saturation within 4 min, after which the monitoring was discontinued. We used the values at 4 min to determine the final concentration and yield of ferrocyanide under various reaction conditions.

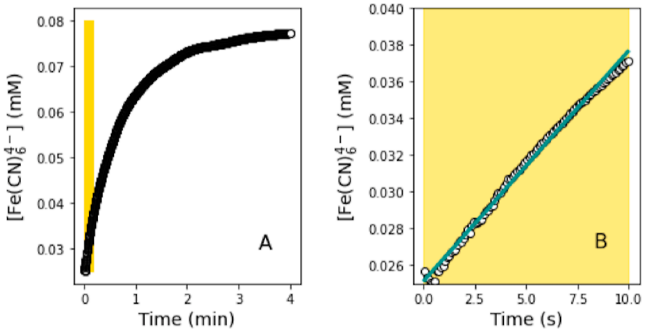

Figure 1. (A) Concentration of ferrocyanide over time after mixing of 0.1 mM Fe(II) and 0.6 mM ΣHCN, unbuffered, at a temperature of 25 °C, calculated from the absorbance feature at 217 nm. The reaction was monitored for four min total. (B) Concentration of ferrocyanide in the first ten s of the reaction [shown as the yellow rectangle in (A)], where the increase in concentration is well-characterized by a linear fit. The slope of the trendline is taken as the rate of the reaction.

We have investigated the rates and yields of ferrocyanide formation under a range of environmental conditions, including pH (≈6−10), temperature (10−70 °C), and concentrations of reactants, by monitoring the appearance of the absorption feature at 217 nm.

pH and Concentration Dependence. The pH of the solution may play a strong role in the formation of ferrocyanide, with more basic solutions known to be more favorable.[25] We sought to systematically study the pH dependence of the reaction in the pH range of 6−10. Note that the speciation of HCN and CN^- varies across the pH range tested (the pK_a of HCN is 9.2 at 25 °C); we refer to the total cyanide concentration as ΣHCN, as defined earlier.

We measured 0.1 mM Fe(II) mixed with 0.2, 0.4, 0.6, and 0.9 mM ΣHCN (Figure 2). We also varied the Fe(II) concentration (0.02, 0.05, 0.1, and 0.2 mM) while holding [ΣHCN] constant at 0.6 mM (Figure 3). All of these solutions were tested at pH 6, 7, 8, 9, and 10 (see Methods for a description of solution preparation and experimental details); all experiments were repeated in triplicates. While this suite is only a subset of possible conditions, with many more possible in planetary environments, it allows for initial investigations into how concentration and pH influence the reaction.

When the Fe(II) concentration was held at 0.1 mM and [ΣHCN] varied from 0.2 to 0.9 mM, we saw that higher concentrations of cyanide generally lead to higher initial rates of ferrocyanide formation (Figure 2A) which is expected. But the pH dependence of these reactions is not monotonic: the

https://doi.org/10.1021/acsearthspacechem.3c00213
ACS Earth Space Chem. 2024, 8, 221−229

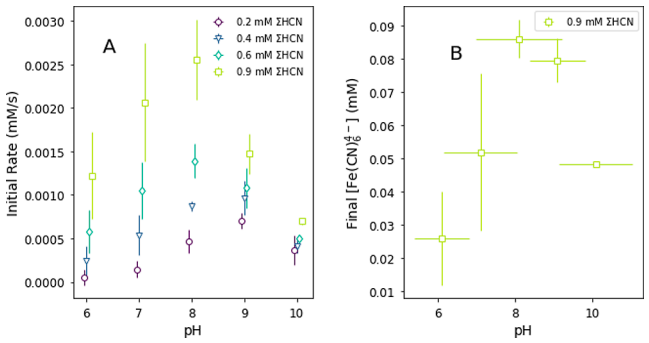

Figure 2. (A) Initial rate of ferrocyanide formation for various pHs and concentrations of ΣHCN, with [Fe(II)] = 0.1 mM and a temperature of 25 °C. Higher concentrations of ΣHCN tend to give higher initial rates, and moderate to slightly alkaline pHs (7−8) are generally the fastest. (B) Final concentration of ferrocyanide as a function of pH and when ΣHCN = 0.9 mM. Yields of ferrocyanide and concentrations are maximal at pH 8−9. All error bars in initial rates and final concentrations represent the 1σ standard deviation from a triplicate set of experiments. The error bars on pH in panel B indicate the change in pH over the course of the reaction and associated uncertainties.

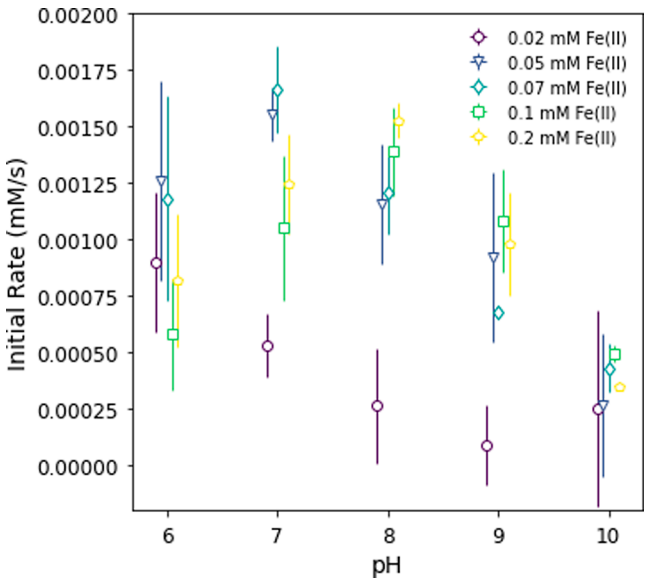

Figure 3. Initial rate of ferrocyanide formation for various pHs and concentrations of Fe(II), with [ΣHCN] = 0.6 mM and a temperature of 25 °C. The moderate to slightly alkaline pHs (7−8) are generally the fastest, and the trend with Fe(II) concentration is less clear. All error bars represent the 1σ standard deviation from a triplicate set of experiments.

more acidic pHs have lower initial rates of ferrocyanide formation, while the maximum values for the initial rate are in the pH 7−9 range. Interestingly, pH 10 did not show a higher rates than pH 9; however, this may be due to more complex processes occurring, such as partial oxidation or speciation of Fe(II) into insoluble ferrous hydroxide at higher pHs. Using solubility data for ferrous hydroxide ($Fe(OH)_2$), we calculated the concentration of Fe(II) that would be in thermodynamic equilibrium with saturated solutions of $Fe(OH)_2$ as a function of pH (see Supporting Information Section S5.) According to these estimates, above pH ≈ 8.5, solutions with 0.1 mM Fe(II) are saturated in insoluble $Fe(OH)_2$. Thus, some portion of Fe(II) used in the pH 9 and 10 experiments could be locked up in $Fe(OH)_2$ and unavailable for forming ferrocyanide. However, the kinetics of these two competing reactions ultimately controls actual concentration. It is unknown which reaction Fe(II) with OH^- to form $Fe(OH)_2$ or Fe(II) with CN^- to form $Fe(CN)_6^{-4}$ would occur more quickly. Both could be occurring at the same time, which would be consistent with our overall observations of decreasing initial rates and final yields of ferrocyanide at the most alkaline pHs tested.

We measured the final yields of ferrocyanide formation in the case of 0.1 mM Fe(II) + 0.9 mM ΣHCN (Figure 2B). Due to experimental challenges, it was not possible to buffer the solutions (buffers interfere with the UV-absorption method of detecting ferrocyanide), leading us to use cyanide itself as the buffer. As expected, the final pH can be significantly different from the initial pH, especially when lower concentrations of cyanide and more acidic initial pHs are used (see Supporting Information Section S6). We find that in the case of 0.9 mM ΣHCN, the pH values before and after the reaction are roughly consistent, within error. The error bars on pH in Figure 2B show the change in pH over the course of the reaction and the associated measurement uncertainties. It should be noted that while the pH may change over the course of the reaction, during the first 10 s when kinetics are quantified, the pH should not have changed significantly.

The influence of [Fe(II)] while cyanide concentration was maintained at 0.6 mM is less clear than the cyanide concentration dependence. However, in general, higher concentrations of Fe(II) lead to similar-to-slightly elevated initial rates of ferrocyanide formation (Figure 3). This may be consistent with the expectation that the order of the reaction is higher in cyanide than in the ferrous iron, as suggested by the stoichiometry and findings of Keefe and Miller (1996). The pH dependence appeared to be consistent with that seen in the experiments with varying concentrations of cyanide.

Our results show that pH plays an important role in the favorability (in terms of both initial rate and final yield) of the formation of ferrocyanide. Acidic pHs are not as favorable as slightly basic to basic pHs, with uncertainty regarding the most basic pHs. When present in concentrations of 0.1 mM Fe(II) + 0.9 mM ΣHCN, the yields of ferrocyanide range from 26 ± 14% (pH 6) to 86 ± 5.8% (pH 9). It is also worth noting that the reaction typically occurs on very fast time scales. For the most favorable pHs, saturation is reached typically on the order of ten s, while even at the less favorable pHs, the reaction seems to proceed as far as it will within minutes.

Temperature Dependence. To assess the temperature dependence of the formation of ferrocyanide, we used unbuffered, pH unadjusted solutions of 0.1 mM Fe(II) + 0.6 mM ΣHCN, held at temperatures from 10 to 70 °C and measured the initial rate of formation and final yield of ferrocyanide. The initial rate of formation (Figure 4A) increases with temperature from 10 to 50 °C but then decreases at 60 and 70 °C. Similarly, the final concentration of ferrocyanide initially increases with temperature but reaches a maximum near 20−25 °C, before falling precipitously at the higher temperatures (Figure 4B). Indeed, at the highest temperature measured (70 °C), the final yield of ferrocyanide is 32.8 ± 0.5%. This value is even less than the yield at the lowest temperature tested of 10 °C (65.5 ± 0.1%). Under the most favorable temperatures, the yield of ferrocyanide is 78.5 ± 0.3% (T = 25 °C).

https://doi.org/10.1021/acsearthspacechem.3c00213
ACS Earth Space Chem. 2024, 8, 221−229

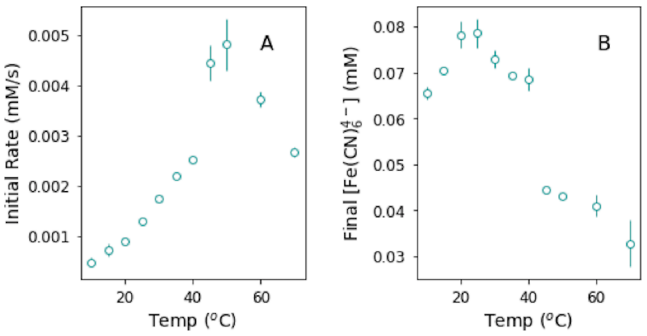

Figure 4. (A) Initial rate of ferrocyanide formation for 0.1 mM Fe(II) + 0.6 mM ΣHCN, pH unadjusted, held at temperatures from 10 to 70 °C. The rate increases from 10 to 50°°C and then drops at 60 and 70 °C. (B) The final concentration of ferrocyanide as a function of temperature is maximized at moderate temperatures (20−25 °C) and decreases significantly at higher temperatures. All error bars represent the 1σ standard deviation from a triplicate set of experiments.

Determining Kinetic Rate Law Parameters. We can next use the experimental data collected to extract parameters for the kinetics of the ferrocyanide formation reaction. The rate law is given as

$$\frac{\mathrm{d}[\mathrm{Fe(CN)}_6^{4-}]}{\mathrm{d}t} = k[\mathrm{Fe(II)}]^m[\Sigma\mathrm{HCN}]^n \quad (4)$$

The parameters m and n indicate the order of the reaction in ferrous iron and cyanide, respectively. From the stoichiometry, one might guess that m = 1 and n = 6, but this is not guaranteed. We calculate k, m, and n for each pH tested, as described in Supporting Information Section S3. Table 1 shows the values and uncertainties determined for these parameters at each pH.

Table 1. Values Determined for Kinetic Parameters m, n, and k, as Described in Supporting Information Section S3

pH	m	n	k (mM^{1-m-n} s^{-1})
6	−0.104 ± 0.181	2.02 ± 0.090	$1.57 \times 10^3 \pm 7.57 \times 10^4$
7	0.103 ± 0.283	1.74 ± 0.048	$4.18 \times 10^3 \pm 3.43 \times 10^3$
8	0.231 ± 0.083	1.20 ± 0.114	$3.90 \times 10^3 \pm 5.26 \times 10^4$
9	0.430 ± 0.236	0.474 ± 0.040	$2.74 \times 10^3 \pm 1.62 \times 10^3$
10	0.216 ± 0.158	0.678 ± 0.131	$3.19 \times 10^4 \pm 5.45 \times 10^5$

Keefe and Miller[25] examined the rate of ferrocyanide formation in several cases; however, their experiments used an excess concentration of Fe(II) and were monitored at an absorbance of 250 nm to lessen the interference of the absorbance from excess Fe(II) at shorter wavelengths. In their pH 6 case, they find n = 3.6 and $k_f = 3.5 \times 10^3$ $\mathrm{M}^{-3.6}$ s^{-1} for the modified rate law

$$\frac{1}{[\mathrm{Fe(II)}]}\left(\frac{\mathrm{d}[\mathrm{Fe(CN)}_6^{4-}]}{\mathrm{d}t}\right) = k_f[\Sigma\mathrm{HCN}]^n \quad (5)$$

For pH 7, Keefe and Miller[25] report n = 2.5 and $k_f = 2.2 \times 10^2$ $\mathrm{M}^{-2.5}$ s^{-1}. Our calculated values for n in the pH 6 and 7 cases are slightly lower than reported by Keefe and Miller[25] (2.02 and 1.74, respectively), but given the experimental differences, this is not surprising. Furthermore, we note that our values are also less than the value of 6 from the stoichiometry of the reaction. Keefe and Miller[25] suggest possible reasons for the lower values of n, including the possibility of formation of $FeOH^+$, alternative pathways for ferrocyanide formation, or that fewer than 6 cyanide ligands are needed on average to flip the complex from high to low spin, which could be the rate-determining step.

DISCUSSION

Implications for Ferrocyanide Formation. We have investigated the formation rates and yields of ferrocyanide under a variety of conditions: from pH 6 to 10, temperatures from 10 to 70 °C, and concentrations of 0.02−0.2 mM Fe(II) and 0.2−0.9 mM ΣHCN. We find generally increasing rates and final concentrations of ferrocyanide when ΣHCN is present in higher concentrations. The most favorable pH values for the reaction are pH ≈ 7−9, with decreasing rates and yields at higher and lower pH values.

For comparison, we also ran geochemical models using the PHREEQC software,[27] which can calculate speciation of chemicals at thermodynamic equilibrium. We specifically calculated the concentration of ferrocyanide expected from 0.1 mM Fe(II) and 0.6 mM ΣHCN, at pHs from 6 to 10 at a temperature of 25 °C (Figure 5A). In general, the experimental

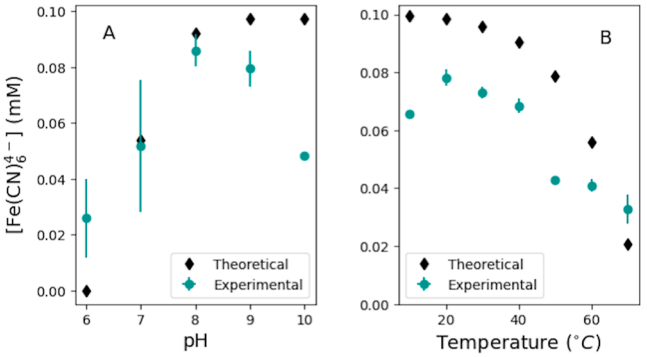

Figure 5. (A) Concentration of ferrocyanide either calculated theoretically from equilibrium thermodynamics (black diamonds) or measured experimentally (teal circles) from solutions of 0.1 mM Fe(II) and 0.6 mM ΣHCN as a function of pH (A) or temperature (B). When pH was varied, the temperature was held constant at 25 °C; for the temperature dependence, solution pHs were unadjusted (pH ≈ 10). The experimental results generally follow the same trend, although theoretical values exceed those measured for higher pHs and lower temperatures.

yields are consistent with theoretical calculations to within a factor of ≈2−3. Notable differences are seen at pH 10, where experimentally, less ferrocyanide was formed than calculated. At pH 6, more ferrocyanide was seen experimentally than is predicted; at pH 7−9, experimental yields are somewhat lower than predicted, but the overall behavior is consistent. We also compare experimental yields and theoretical calculations for varying temperatures, for pH 10 solutions (Figure 5B). The experimental yields are somewhat reduced from the theoretical predictions, especially at lower temperatures. It is possible that further equilibration of experimental solutions would bring ferrocyanide concentrations closer to the predicted values. Another explanation for the observed differences could be due to solubility issues in the experiments, particularly that of Fe(II). Overall, the fact that experimental concentrations are fairly consistent with theoretical predictions improves confidence in the accuracy of our measurements.

https://doi.org/10.1021/acsearthspacechem.3c00213
ACS Earth Space Chem. 2024, 8, 221−229

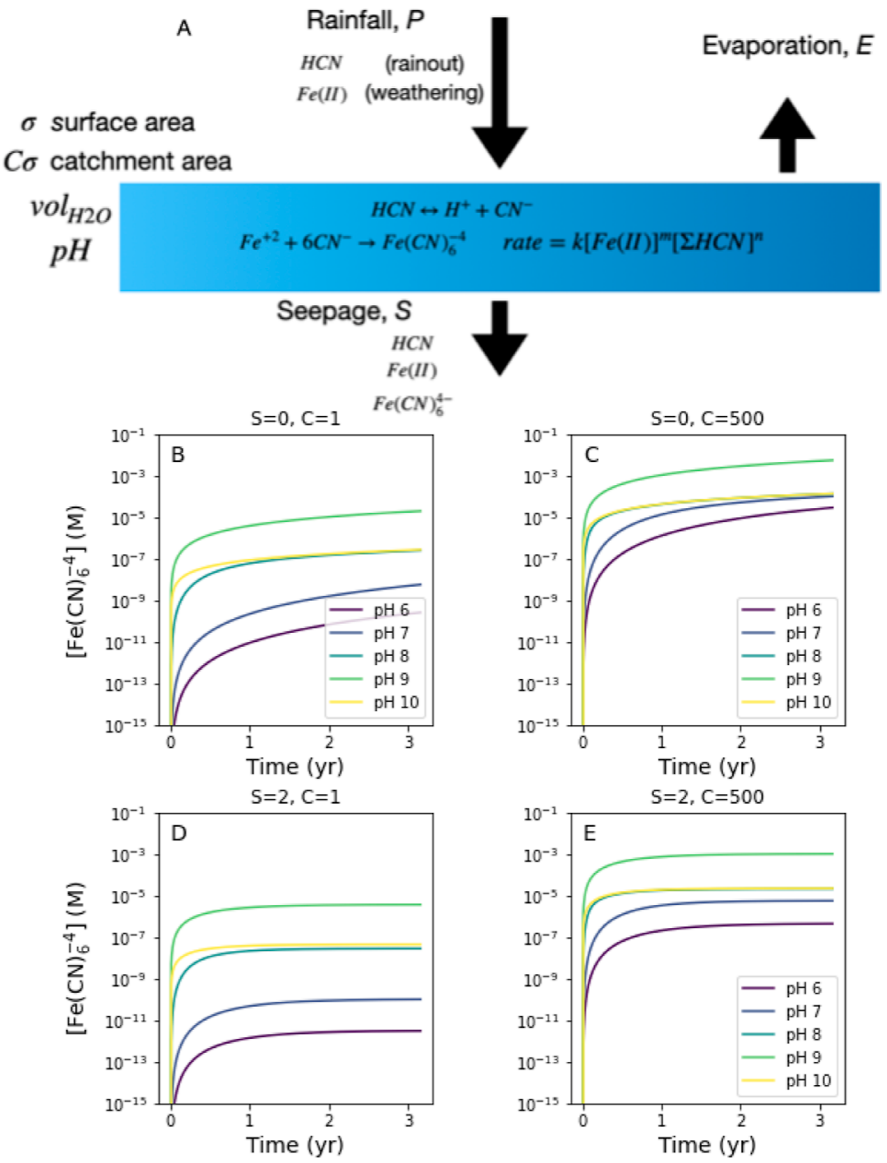

Figure 6. (A) Schematic of lake model. (B–E) Concentrations of ferrocyanide in model lake scenarios, including closed basin [i.e., S = 0, (B,C)] and maximum seepage [S = 2, (D,E)]. The catchment area is taken as either the geometrical surface area of the lake [C = 1, (B,D)] or the maximum range considered [C = 500, (C,E)]. In the most favorable case (panel C), concentrations of 1 mM $Fe(CN)_6^{-4}$ are attained within 1000 years for all pH values except 6.

In addition to the role pH plays in the formation of ferrocyanide, we found that the temperature can play a strong role in the reaction, especially affecting the final concentration. While the rate of the reaction generally increased with temperature up to 50 °C, the final concentration of ferrocyanide peaked at 25 °C, before falling significantly at higher temperatures. This indicates that ferrocyanide may have a lower stability at higher temperatures.

Overall, the most favorable conditions for ferrocyanide formation appear to be moderate temperatures and slightly alkaline conditions (pH 8–9). However, we do see ferrocyanide form robustly across all of the parameters we tested, though with smaller overall yields at the less favorable conditions (e.g., acidic/neutral pH and higher temperatures).

Example Lake Box Model. With these experimental data, we can construct toy box model calculations to simulate conditions on early Earth. In a simple scenario, we consider a shallow lake with a depth of 1 m and a fiducial volume of 10^6 L (see Figure 6A for a schematic overview). Postimpact atmospheres can be reducing enough to allow for significant formation of HCN in the atmosphere, which can enter surface waters by rainout or partitioning due to Henry's law dissolution.[14,15] Wogan et al.[15] estimate a rainout flux of $r_{HCN} = 10^9$ molecules cm^{-2} s^{-1} for global postimpact atmospheres with mole ratios of $CH_4/CO_2 > 0.1$, which can be achieved by impactors >570–1330 km diameter. On the early Earth, reduced iron (Fe(II)) would likely be available as the environment would have been largely anoxic. Rainwater dissolves atmospheric CO_2 to generate carbonic acid, which weathers soils and rocks to release Fe(II) into the environment. The weathering process depends on temperature and the amount of CO_2 in the atmosphere.[28,29] Various studies have calculated Fe(II) concentrations in anoxic environments in Earth's past. Garrels[30] estimated Fe(II) concentrations of ≈0.7 mM in river water flowing over basalt. Hao et al.[31] found 0.099 mM Fe(II) in water that weathered olivine basalts. While the

https://doi.org/10.1021/acsearthspacechem.3c00213
ACS Earth Space Chem. 2024, 8, 221–229

precise amounts of Fe(II) available in anoxic geochemical environments vary, we estimate a fiducial concentration of 0.1 mM Fe(II), following Toner and Catling.[26] This iron concentration is not dissimilar to that at some anoxic lower layers of lakes at quasi-neutral pH, e.g., 11.11 mg/L Fe(II) (or 0.2 mM Fe(II)) found at a depth of 20 m in Lake La Cruz, Spain, at pH 6.6.[32] We then assess the dependence of our results on the assumed concentrations of Fe(II).

The rate of deposition of a molecule X in molecules s^{-1} from rainfall is given by

$$f_{\text{rainfall},X} = [X]PC\sigma \tag{6}$$

where P is the rainfall rate (m s^{-1}), $[X]$ is the concentration of a given molecule (molecules m^{-3}), σ is the surface area of the lake (m^2), and C is a constant allowed to vary to account for the range of possible catchment areas of lakes (unitless) since these may be many times the area of the lake itself.[33] We explore a range of C = 1−500, with the lower limit corresponding to the conservative case of the catchment area being equal to the physical surface area of the lake. The upper limit corresponds to the total catchment area from a sample of 236 ponds, as determined by Davies et al.[33]

Water will seep out of a lake, resulting in a loss of dissolved chemicals from the system. The seepage rate S of lakes is variable: we explore a range of S = 0−2 m/year, following Ranjan et al. (2023).[34] Closed basin lakes, meaning lakes without outlet streams, have no loss due to seepage (S = 0), and water loss is only due to evaporation in these cases, which allows for increasing concentrations of dissolved chemical species (e.g., Toner and Catling[26]). The upper limit for seepage rate considered here, S = 2 m/yr corresponds to the estimates for Lake Castor, located in Washington[35] and fishponds near Auburn, Alabama.[36,37]

The rate of loss of species X due to seepage is given by

$$f_{\text{seepage,X}} = S[X]\sigma \tag{7}$$

The evaporation rate E (in m yr^{-1}) is a function of surface temperature (K), following Pearce et al.[37] and Boyd[36]

$$E = -0.12 + 0.06(T_{\text{surf}} - 273.15) \tag{8}$$

We assume that the total volume of the lake is not changing with time, meaning that the rainfall rate (here, implicitly including runoff from the surrounding catchment) is equal to the sum of seepage and evaporation. Positive seepage is implicitly assumed to be a net groundwater outflow, where groundwater outflow exceeds inflow.

$$P = S + E \tag{9}$$

Additionally, we use our experimentally determined rate laws for various pHs to calculate the rate of loss of Fe(II) and cyanide and the rate of production of ferrocyanide

$$\text{rate}_{\text{pHX}} = k_{\text{pHX}}[\text{Fe(II)}]^{m_{\text{pHX}}}[\Sigma\text{HCN}]^{n_{\text{pHX}}} \tag{10}$$

where rate_{pHX} is the rate of formation of ferrocyanide at a selected pH (6, 7, 8, 9, or 10), k_{pHX} is the derived rate constant at each pH, and m_{pHX} and n_{pHX} are the reaction orders in Fe(II) and ΣHCN, respectively, determined at each pH.

We use the total HCN concentration, e.g., $[\Sigma\text{HCN}] = [\text{HCN}] + [\text{CN}^-]$, in the rate equation, because as CN^- is consumed by the formation reaction, it will be replenished by equilibration from HCN, as calculated by the Henderson−Hasselbach eq 11, according to the pH of the body of water.

$$\text{pH} = \text{p}K_a + \log_{10}\left(\frac{[\text{CN}^-]}{[\text{HCN}]}\right) \tag{11}$$

where the $\text{p}K_a$ of HCN is 9.2 at 25 °C.

The differential equations used to calculate the change in concentration (in molecules/s) of the three species, Fe(II), ΣHCN, and Fe(CN)_6^{-4} are

$$\frac{\text{d}[\Sigma\text{HCN}]}{\text{d}t} = r_{\text{HCN}}C\sigma - f_{\text{seepage},\Sigma\text{HCN}} - 6\text{rate}_{\text{pHX}}N_{\text{A}}V_{\text{lake}} \tag{12}$$

$$\frac{\text{d}[\text{Fe(II)}]}{\text{d}t} = f_{\text{rainfall,Fe(II)}} - f_{\text{seepage,Fe(II)}} - \text{rate}_{\text{pHX}}N_{\text{A}}V_{\text{lake}} \tag{13}$$

$$\frac{\text{d}[\text{Fe(CN)}_6^{-4}]}{\text{d}t} = \text{rate}_{\text{pHX}}N_{\text{A}}V_{\text{lake}} - f_{\text{seepage,Fe(CN)}_6^{-4}} \tag{14}$$

where all terms have been converted to units of molecules s^{-1} (N_{A} is Avogadro's number, 6.02×10^{23}). Here, r_{HCN} is the rainout rate of HCN from the atmosphere after a reducing after (taken as 10^9 molecules s^{-1} cm^{-2},[15]). Rainfall is presumed to weather the catchment area soil or rock to release Fe(II) at a rate of $f_{\text{rainfall,Fe(II)}}$.

We numerically solve for the concentrations of each species as a function of time for the cases of (i) S = 0, C = 1; (ii) S = 0, C = 500; (iii) S = 2, C = 1; and (iv) S = 2, C = 500 (Figure 6, B−E). In the closed-basin (S = 0) cases, the concentration of ferrocyanide continues to increase with time, while in the maximum seepage (S = 2) case, steady-state concentrations are reached within a few years. In the cases with a higher catchment area, the concentrations of ferrocyanide are several orders of magnitude larger than in the C = 1 case. Finally, pH 9 allows maximum ferrocyanide concentrations, while the more acidic pHs show significantly less ferrocyanide formation. Under the most favorable cases (S = 0, C = 500), concentrations of $[\text{Fe(CN)}_6^{-4}]$>1 μM are achieved within 1 year for all pHs (see Table 2 for concentrations for each pH).

Table 2. $[\text{Fe(CN)}_6^{-4}]$ for Various pHs at t = 1 year in the S = 0, C = 500 Case

pH	$[\text{Fe(CN)}_6^{-4}]$ (μM)
6	1.30
7	13.5
8	42.1
9	1080
10	43.5

In these models, we use a surface temperature of 288 K, corresponding to the temperature at which the experiments to determine the rate equations were conducted. However, the surface temperature may be hotter in a postimpact atmosphere. Wogan et al.[15] predict a surface temperature of >360 K in postimpact atmospheres, albeit with the caveat that the albedo effect of clouds and haze, which are not fully modeled, could lower this temperature. Given the temperature dependence observed experimentally, where elevated temperatures result in significantly less ferrocyanide formed, it is possible that ferrocyanide formation rates in such hot environments would be diminished, but perhaps compensated for by elevated weathering of Fe(II) given that weathering rates have an exponential dependence on temperature.[28]

https://doi.org/10.1021/acsearthspacechem.3c00213
ACS Earth Space Chem. 2024, 8, 221−229

There are a number of free parameters set to fiducial values in our sample lake models above. We explored plausible ranges of catchment areas (C = 1−500) and seepage rates (S = 0−2 m/yr) but selected fiducial values for the depth and volume of the lake, as well as the concentration of Fe(II) from rainfall and subsequent weathering. We assess the sensitivity of our results to these assumptions in Supporting Information Section S4.

Caveats and Further Reactions. These calculations offer simple models of ferrocyanide production and accumulation in lake environments, but we have made a number of assumptions. In addition to the free parameters discussed above, uncertainties exist in various aspects of the rate laws that we have determined experimentally and used in these models. For example, we assume that the rate laws hold at the concentrations investigated here, which, in some cases, are significantly smaller than those used in laboratory experiments. Our experimental results did not determine the effect of ionic strength on the rates of ferrocyanide formation, so caution should be used when extrapolating results to waters containing other ions in abundance. We also do not quantify how different temperatures affect the model results. From our experimental investigation of the temperature dependence, higher temperatures result in significantly lower yields of ferrocyanide. However, determining the kinetic parameters (i.e., k, m, and n) for all pHs as a function of temperature is outside the scope of this work.

These models assume no sinks for the chemical species other than seepage and the reaction to form ferrocyanide. In actual geochemical scenarios, other sinks are likely to exist. Cyanide undergoes hydrolysis[22] and possibly oligomerization,[38] which we have assumed is not occurring to significant extents under the reaction conditions we have studied here. Under other conditions (higher concentrations, longer time scales, etc.), these reactions may become more important, perhaps influencing both the kinetic parameters and the chemical network of reactions occurring. Furthermore, Fe(II) can react with other chemical constituents, especially to form insoluble minerals, including ferrous hydroxide ($Fe(OH)_2$) and siderite ($FeCO_3$). In geochemical scenarios where OH^-, CO_3^{-2}, etc., are present in large quantities, these could act as limits on Fe(II) solubility, which could potentially limit the amount of ferrocyanide that can be formed.

Another caveat is that ferrocyanide degrades under UV and near-UV light,[24] which is likely to have been present on the early Earth. We also neglect the long-term stability of ferrocyanide in the absence of UV light. It is possible that ferrocyanide concentrations will reach an equilibrium where production is balanced by destruction. The short duration of our experiments here to monitor formation rates may not take this into account. Furthermore, such equilibrium concentrations are likely to depend on environmental conditions, such as temperature, pH, and concentration, which would all need to be determined experimentally. Additionally, this calculation assumes that the rate-limiting step for the formation of ferrocyanide is the reaction between Fe(II) and cyanide. However, if the rate of this reaction is faster than the release of Fe(II) and cyanide to the lake, then this assumption may not hold. Our model assumes that the volume of the lake is not changing and that ferrocyanide does not have the opportunity to precipitate out of solution. In cases where evaporation occurs, ferrocyanide can precipitate as various salts and potentially accumulate and stockpile in this manner (see Toner and Catling[26] and Sasselov et al.[23] for further discussion). In the planetary scenario, it is likely that there will be depth-dependent variations in the concentrations of ferrocyanide as cyanide rains out to form ferrocyanide, UV light is acting to degrade ferrocyanide near the surface, further reactions are occurring in the aqueous medium, and precipitation is occurring to allow complexes to come out of solution.

Full modeling of all of these considerations is beyond the scope of this largely experimental study. Therefore, we caution that these lake models are only simple example calculations to provide some context for possible time scales and concentrations but that these values may fluctuate significantly under different conditions or when a more complete model incorporating further complexities is implemented. We hope future work will incorporate additional sinks for ferrocyanide and potential storage/protective mechanisms from degradation, such as shielding from UV light or precipitation during prolonged drying periods. Nevertheless, our results suggest that ferrocyanide can accumulate to potentially significant concentrations over reasonable time scales (i.e., tens to hundreds of years), with the most favorable scenarios in closed-basin lakes with little to no seepage. The most favorable pH values for ferrocyanide formation are moderately alkaline (pH 8−9).

CONCLUSIONS

In this study, we experimentally investigated the formation of ferrocyanide from Fe(II) and cyanide under a range of parameters, including the pH, temperature, and concentration. We determined the initial rates of the reaction as well as final yields. Our results show that the formation of ferrocyanide is most favorable at slightly alkaline conditions (e.g., pH 8−9) and moderate temperatures (≈20−25 °C), with acidic pHs and higher temperatures being particularly inefficient for the reaction. These experimental results can be used in simple models of lakes on the early Earth to calculate possible concentrations of ferrocyanide and the relevant time scales for ferrocyanide accumulation. While these models depend on assumptions about the lake, we find that ferrocyanide can accumulate to potentially significant concentrations (e.g., >0.1 mM) on time scales of tens of years under the most favorable conditions. This suggests that prebiotic chemistry making use of ferrocyanide could be accessible under a range of conditions in surface waters with a source of Fe(II) in contact with an atmosphere containing HCN, for example, after a large impact, with the caveat that the elevated temperatures likely in postimpact conditions may reduce the efficiency of ferrocyanide formation. Improving these models with additional sinks, the possibility of precipitation of relevant ferrocyanide salts, and assessing the kinetics of both ferrocyanide production and destruction will further aid our understanding of the plausibility and the necessary conditions for ferrocyanide- and cyanide-dependent prebiotic chemistry.

EXPERIMENTAL SECTION

Sodium cyanide (98%) was purchased from Thermo-Fisher, and iron(II) chloride (99%) was purchased from Sigma-Aldrich. Appropriate amounts of the chemicals were weighed out as solids and transferred to a Coy Laboratories Anaerobic Chamber (98% N_2, 2% H_2). Stock solutions of 1 mM Fe(II) and 1 mM ΣHCN were made anaerobically. The pH of the cyanide stock solution was checked by using pH strips and

https://doi.org/10.1021/acsearthspacechem.3c00213
ACS Earth Space Chem. 2024, 8, 221−229

adjusted by using NaOH or HCl solutions. Stock solutions of 1 mM ΣHCN were made at pH 6, 7, 8, 9, and 10, with the pH monitored using pH strips.

The pH-adjusted ΣHCN stock solutions were diluted to the appropriate concentrations of cyanide (0, 0.2, 0.4, 0.6, and 0.9 mM) and placed in quartz cuvettes with septa-containing screw-on tops (Starna Cells Part #1-Q-10-GL14-S). Gas tight syringes (Hamilton, Part #7649-01) were prepared with the appropriate volume of Fe(II) stock solution. When an experiment was conducted, the cuvette and syringe were removed from the Anaerobic Chamber. The cuvette was placed in an Agilent Cary-60 UV−vis spectrophotometer set to monitor kinetics at 217 nm (the absorption peak of ferrocyanide) for 4 min. The syringe containing the Fe(II) solution was injected into the cuvette, and the absorbance measurement started immediately thereafter.

For temperature-dependent experiments, the same preparation procedures were followed, and a Peltier chiller was used to control the temperature of the cuvette holder. The cuvette containing cyanide solution was allowed to equilibrate to the given temperature for at least five min before initiating the reaction and measuring the kinetics.

Absorption at 217 nm was converted into a concentration of ferrocyanide by using a standard curve constructed from the absorption of solutions with known concentrations. To determine the rate of the reaction, the concentration as a function of time over the first ten s was fit with a linear trendline. The final concentration was determined at the end of the 4 min scan. All experiments were repeated in triplicate; error bars are the 1σ standard deviation from the triplicate set. See Supporting Information Section S2 for details on measurements and analysis procedures.

Safety Statement. The experimental work carried out in this study used sodium cyanide, a toxic substance. To safely carry out this work, all cyanide solutions were prepared in an anaerobic glovebox and then transferred to gastight quartz cuvettes. To measure the final pH of samples, the gastight cuvettes were moved to a fume hood where the pH meter was set up. Solutions were uncapped underneath the fume hood, and pH was measured. This ensured that the user was never exposed to cyanide-containing solutions or vapors during the course of the experiment. Appropriate measures were used for disposing of cyanide-containing waste according to the Environmental Health and Safety Office at the University of Washington.

■ ASSOCIATED CONTENT

Supporting Information

The Supporting Information is available free of charge at https://pubs.acs.org/doi/10.1021/acsearthspacechem.3c00213.

General methods; determination of rates; kinetics analysis—determination of k, m, and n; lake model sensitivity tests; solubility of Fe(II) and formation of $Fe(OH)_2$; and final pH values during experiments (PDF)

Experimental raw data (ZIP)

■ AUTHOR INFORMATION

Corresponding Author

Zoe R. Todd − *Department of Earth and Space Sciences, University of Washington, Seattle, Washington 98195, United States; Departments of Chemistry and Astronomy, University of Wisconsin-Madison, Madison, Wisconsin 53706, United States;* orcid.org/0000-0001-6116-4285; Email: zrtodd@wisc.edu

Authors

Nicholas F. Wogan − *Department of Earth and Space Sciences, University of Washington, Seattle, Washington 98195, United States;* orcid.org/0000-0002-0413-3308

David C. Catling − *Department of Earth and Space Sciences, University of Washington, Seattle, Washington 98195, United States;* orcid.org/0000-0001-5646-120X

Complete contact information is available at: https://pubs.acs.org/10.1021/acsearthspacechem.3c00213

Notes

The authors declare no competing financial interest.

■ ACKNOWLEDGMENTS

The authors thank P. Rimmer and S. Ranjan for useful discussions and helpful ideas. The authors would also like to thank the two reviewers for comments and suggestions in improving the manuscript. Support for this work was provided by to by NASA through the NASA Hubble Fellowship Program (grant #HST-HF2-51471 to Z.R.T.) awarded by the Space Telescope Science Institute, which is operated by the Association of Universities for Research in Astronomy, Inc., for NASA under contract NAS5-26555. The authors acknowledge funding from the Simons Foundation (grant #511570 to D.C.C.). The authors would also like to acknowledge support from the University of Washington Astrobiology Program.

■ REFERENCES

(1) Oro, J. Synthesis of adenine from ammonium cyanide. *Biochem. Biophys. Res. Commun.* **1960**, *2*, 407−412.

(2) Miller, S. L. The mechanism of synthesis of amino acids by electric discharges. *Biochim. Biophys. Acta* **1957**, *23*, 480−489.

(3) Miller, S. L.; Cleaves, H. J. Prebiotic chemistry on the primitive Earth. *Syst. Biol.* **2006**, *1*, 3−56.

(4) Patel, B. H.; Percivalle, C.; Ritson, D. J.; Duffy, C. D.; Sutherland, J. D. Common origins of RNA, protein and lipid precursors in a cyanosulfidic protometabolism. *Nat. Chem.* **2015**, *7*, 301−307.

(5) Xu, J.; Ritson, D. J.; Ranjan, S.; Todd, Z. R.; Sasselov, D. D.; Sutherland, J. D. Photochemical reductive homologation of hydrogen cyanide using sulfite and ferrocyanide. *Chem. Commun.* **2018**, *54*, 5566−5569.

(6) Yi, R.; Hongo, Y.; Yoda, I.; Adam, Z. R.; Fahrenbach, A. C. Radiolytic Synthesis of Cyanogen Chloride, Cyanamide and Simple Sugar Precursors. *ChemistrySelect* **2018**, *3*, 10169−10174.

(7) Yi, R.; Tran, Q. P.; Ali, S.; Yoda, I.; Adam, Z. R., II; Cleaves, H. J.; Fahrenbach, A. C. A continuous reaction network that produces RNA precursors. *Proc. Natl. Acad. Sci. U.S.A.* **2020**, *117*, 13267−13274.

(8) Becker, S.; Thoma, I.; Deutsch, A.; Gehrke, T.; Mayer, P.; Zipse, H.; Carell, T. A high-yielding, strictly regioselective prebiotic purine nucleoside formation pathway. *Science* **2016**, *352*, 833−836.

(9) Liu, Z.; Wu, L.-F.; Bond, A. D.; Sutherland, J. D. Photoredox chemistry in the synthesis of 2-aminoazoles implicated in prebiotic nucleic acid synthesis. *Chem. Commun.* **2020**, *56*, 13563−13566.

(10) Teichert, J. S.; Kruse, F. M.; Trapp, O. Direct prebiotic pathway to DNA nucleosides. *Angew. Chem. Int. Ed.* **2019**, *58*, 9944−9947.

(11) Kim, H.-J.; Benner, S. A. Prebiotic stereoselective synthesis of purine and noncanonical pyrimidine nucleotide from nucleobases and phosphorylated carbohydrates. *Proc. Natl. Acad. Sci. U.S.A.* **2017**, *114*, 11315−11320.

(12) Zahnle, K. J. Photochemistry of CH4 and HCN in the primitive atmosphere. *Origins Life Evol. Biospheres* **1986**, *16*, 188−189.
(13) Tian, F.; Kasting, J. F.; Zahnle, K. Revisiting HCN formation in Earth's early atmosphere. *Earth Planet. Sci. Lett.* **2011**, *308*, 417−423.
(14) Zahnle, K. J.; Lupu, R.; Catling, D. C.; Wogan, N. Creation and evolution of impact-generated reduced atmospheres of early Earth. *Planet. Sci. J.* **2020**, *1* (1), 11.
(15) Wogan, N. F.; Catling, D. C.; Zahnle, K. J.; Lupu, R. Origin of Life Molecules in the Atmosphere after Large Impacts on the Early Earth. *Planet. Sci. J.* **2023**, *4* (9), 169.
(16) Stribling, R.; Miller, S. L. Energy yields for hydrogen cyanide and formaldehyde syntheses: the HCN and amino acid concentrations in the primitive ocean. *Origins Life Evol. Biospheres* **1987**, *17*, 261−273.
(17) Chameides, W. L.; Walker, J. C. G. Rates of fixation by lightning of carbon and nitrogen in possible primitive atmospheres. *Orig. Life* **1981**, *11*, 291−302.
(18) Ferus, M.; Kubelik, P.; Knizek, A.; Pastorek, A.; Sutherland, J.; Civis, S. High energy radical chemistry formation of HCN-rich atmospheres on early Earth. *Sci. Rep.* **2017**, *7*, 6275.
(19) Parkos, D.; Pikus, A.; Alexeenko, A.; Melosh, H. J. HCN production via impact ejecta reentry during the Late Heavy Bombardment. *J. Geophys. Res.: Planets* **2018**, *123*, 892−909.
(20) Benner, S. A.; Bell, E. A.; Biondi, E.; Brasser, R.; Carell, T.; Kim, H.-J.; Mojzsis, S. J.; Omran, A.; Pasek, M. A.; Trail, D. When did life likely emerge on Earth in an RNA-first process? *ChemSystemsChem* **2020**, *2* (2), No. e1900035.
(21) Todd, Z. R.; Oberg, K. I. Cometary delivery of hydrogen cyanide to the early Earth. *Astrobiology* **2020**, *20*, 1109−1120.
(22) Miyakawa, S.; James Cleaves, H.; Miller, S. L. The cold origin of life: A. Implications based on the hydrolytic stabilities of hydrogen cyanide and formamide. *Origins Life Evol. Biospheres* **2002**, *32*, 195−208.
(23) Sasselov, D. D.; Grotzinger, J. P.; Sutherland, J. D. The origin of life as a planetary phenomenon. *Sci. Adv.* **2020**, *6* (6), No. eaax3419.
(24) Todd, Z. R.; Lozano, G. G.; Kufner, C. L.; Sasselov, D. D.; Catling, D. C. Ferrocyanide survival under near ultraviolet (300−400 nm) irradiation on early Earth. *Geochim. Cosmochim. Acta* **2022**, *335*, 1−10.
(25) Keefe, A. D.; Miller, S. L. Was ferrocyanide a prebiotic reagent? *Origins Life Evol. Biospheres* **1996**, *26*, 111−129.
(26) Toner, J. D.; Catling, D. C. Alkaline lake settings for concentrated prebiotic cyanide and the origin of life. *Geochim. Cosmochim. Acta* **2019**, *260*, 124−132.
(27) Appelo, C. A.; Postma, D. *Geochemistry, Groundwater and Pollution*, 2nd ed.; CRC Press, 2005.
(28) Walker, J. C. G.; Hays, P. B.; Kasting, J. F. A negative feedback mechanism for the long-term stabilization of Earth's surface temperature. *J. Geophys. Res.: Oceans* **1981**, *86*, 9776−9782.
(29) Krissansen-Totton, J.; Catling, D. C. Constraining climate sensitivity and continental versus seafloor weathering using an inverse geological carbon cycle model. *Nat. Commun.* **2017**, *8*, 15423.
(30) Garrels, R. M. A model for the deposition of the microbanded precambrian iron formations. *Am. J. Sci.* **1987**, *287*, 81−106.
(31) Hao, J.; Sverjensky, D. A.; Hazen, R. M. A model for late Archean chemical weathering and world average river water. *Earth Planet. Sci. Lett.* **2017**, *457*, 191−203.
(32) Rodrigo, M. A.; Miracle, M.; Vicente, E. The Meromictic Lake La Cruz (Central Spain). Patterns of Stratification. *Aquat. Sci.* **2001**, *63*, 406−416.
(33) Davies, B.; Biggs, J.; Williams, P.; Lee, J.; Thompson, S. A comparison of the catchment sizes of rivers, streams, ponds, ditches and lakes: implications for protecting aquatic biodiversity in an agricultural landscape. *Hydrobiologia* **2008**, *597*, 7−17.
(34) Ranjan, S.; Abdelazim, K.; Lozano, G. G.; Mandal, S.; Zhou, C. Y.; Kufner, C. L.; Todd, Z. R.; Sahai, N.; Sasselov, D. D. Geochemical and Photochemical Constraints on S[IV] Concentrations in Natural Waters on Prebiotic Earth. *AGU Adv.* **2023**, *4*, No. e2023AV000926.
(35) Steinman, B. A.; Rosenmeier, M. F.; Abbott, M. B.; Bain, D. J. The isotopic and hydrologic response of small, closed-basin lakes to climate forcing from predictive models: Application to paleoclimate studies in the upper Columbia River basin. *Limnol. Oceanogr.* **2010**, *55*, 2231−2245.
(36) Boyd, C. E. Hydrology of small experimental fish ponds at Auburn, Alabama. *Trans. Am. Fish. Soc.* **1982**, *111*, 638−644.
(37) Pearce, B. K. D.; Pudritz, R. E.; Semenov, D. A.; Henning, T. K. Origin of the RNA World: The fate of nucleobases in warm little ponds. *Proc. Natl. Acad. Sci. U.S.A.* **2017**, *114*, 11327−11332.
(38) Oro, J.; Kimball, A. P. Synthesis of purines under possible primitive Earth conditions. I. Adenine from hydrogen cyanide. *Arch. Biochem. Biophys.* **1961**, *94*, 217−227.

https://doi.org/10.1021/acsearthspacechem.3c00213
ACS Earth Space Chem. 2024, 8, 221−229